Energy Analysis on the Effect of Magnetic Field on Nanoparticles Fluidization

Hamed Hoorijani [ID], Navid Mostoufi * [ID], Reza Zarghami [ID]

1. Multiphase Systems Research Lab, School of Chemical Engineering, College of Engineering, University of Tehran, Tehran, Iran. E-mail: hoorijani@ut.ac.ir
2. Multiphase Systems Research Lab, School of Chemical Engineering, College of Engineering, University of Tehran, Tehran, Iran. E-mail: mostoufi@ut.ac.ir
3. Multiphase Systems Research Lab, School of Chemical Engineering, College of Engineering, University of Tehran, Tehran, Iran. E-mail: rzarghami@ut.ac.ir

ARTICLE INFO	ABSTRACT
	Effects of magnetic field strength and direction were studied on the fluidization of titanium oxide nanoparticles (anatase phase) with ferromagnetic iron (III) oxide nanoparticles. The main hydrodynamic structures were defined and studied using wavelet transform. Energy analysis was used to study the effect of the field direction and strength on fluidization. The results suggested that mesostructures (agglomerates) have the most effect on the nanoparticle fluidization characteristics. Higher energy at high field strength for upward direction, suggests more intense interaction between agglomerates in the bed for nanoparticles that result in a more stochastic pattern and lower ABF regime characteristics. Downward direction at low magnetic field strength shows improving the fluidization quality by the effect of the vibration of the solenoid. It was observed that at low field strength, vibration has a major effect on fluidization than the magnetic force. At high magnetic field strength, as the magnetic force becomes stronger, the downward field decreases the energy of finer structures (agglomerates) which leads to less movement and resistance against fluidization.

Introduction

Fluidized beds are one of the most common equipment in multiphase flows. Fluidization is a popular method to process powders, owing to its distinctive transport phenomena features and its wide range of applications across several chemical industries. Various industries have used nanopowders in recent years because of their unique properties [1]. Nanopowders exhibit excellent mass-heat transfer characteristics, which makes them suitable for a variety of applications. Even though the fluidization of these powders has great advantages, it suffers from disadvantages, such as channeling and plugging that restrict its performance [2]. Nanopowders are classified as Group C of Geldart's classification of powders [3, 4]. This group of powders has high cohesive forces between the particles, and they mainly exist in the form of agglomerates [5-7]. Agglomeration of these particles decreases the contact surface between the particles and the fluid, decreasing yields and conversion in chemical processes.

---

* Corresponding Author: N. Mostoufi (E-mail address: mostoufi@ut.ac.ir)

Agglomerate particulate fluidization (APF) and agglomerate bubbling fluidization (ABF) are two types of flow regimes in the fluidization of these powders [8, 9]. As opposed to the ABF, the APF regime has a uniform and higher bed expansion, while ABF has a low bed expansion and larger bubbles during fluidization. The structure of agglomerates in the APF regime has a porous structure characterized by a multistep formation mechanism that results in smaller agglomerates than those in the ABF regime [8]. The fluidizing of these powders may involve some difficulties, and assisting methods have been proposed to alleviate these difficulties as well as to improve the quality of fluidization. Recent studies have indicated that employing internal or external assistance can reduce fluidization velocity, mean agglomerate size, and enhance the fluidization quality [2]. External methods mostly include mechanical vibration [10, 11], electric field [12], and magnetic field [13]. One of the most suitable methods for improving the fluidization quality is the use of the magnetic field, which has a direct impact on the magnetic particles in the bed and can enhance the mixing in the bed.

Hydrodynamics of fluidized beds has been studied using a variety of techniques. It has been demonstrated that measuring and analyzing pressure fluctuations is an effective technique for identifying the key hydrodynamic phenomena in the bed [14]. Due to its simplicity and ease of industrial application, it is one of the most common methods for studying flow dynamics. These nonlinear time series of pressure fluctuations can be analyzed in time, frequency, and state-space domains [15]. The results from these methods provide valuable insights into the hydrodynamics of fluidized beds, as well as the movement of bubbles and particles. The wavelet transform has been used to detect different phenomena in fluidized beds based on pressure fluctuations. In fluidized beds, large bubbles constitute large phenomena with low frequencies in the power spectrum density (PSD) analysis of the pressure fluctuations that constitute the macrostructure. In the PSD, smaller bubbles and agglomerates display higher frequency and are classified as mesostructure. Microstructures are particle movements and noise in the measurement system [16]. Tamadondar et al. [16] studied the fluidization of silica nanoparticles using the wavelet transform. They analyzed pressure fluctuation signals in frequency and time-frequency domains and identified the main hydrodynamic structures of nanoparticle fluidization using PSD and energy analyses. They showed by studying the energy distribution of sub-signals that mesostructures have the most effect in nanoparticle fluidization. Farahani et al. [17] investigated the characteristics of each flow regime by computational fluid dynamics- discrete element method (CFD-DEM). They showed that the ABF regime has a higher value of axial and radial dispersion coefficient and better mixing quality. Liu and Wang [18] studied the effect of the initial height of the bed of nanoparticles on fluidization. They stated that the minimum fluidization velocity significantly decreases with the increase of the initial bed height for silica oxide nanoparticles. They also observed that most of the particles become fluidized at the dense bottom region of the bed. The mean diameter of agglomerates in this region increases with the initial bed height and the superficial gas velocity.

This study was conducted to investigate the effect of magnetic field strength and its direction on the fluidization of mixtures of titanium oxide and iron oxide (used as the magnetic agent) nanoparticles. In this study, wavelet transform was used to determine the main hydrodynamic structures (i.e., bubbles and agglomerates) in the bed. The effect of both intensity and direction of the magnetic field on the main phenomena in the bed was examined through the analysis of the energy of pressure fluctuation signals.

Experiments

Fig. 1 shows the schematic of the experimental set-up, which is a cylindrical column with an inner diameter of 26 mm and a height of 80 mm, made of quartz. A plastic wind box filled

with 5 mm plastic balls was used to ensure efficient distribution of the gas. A sintered porous metal distributor plate with a porosity of 60% and a thickness of 1 mm was used above the wind box (MOTT corp.). Dry nitrogen was supplied by a cylinder as the fluidizing gas. To control the flow of the gas into the bed, a digital mass flow controller (MC-5SLPM-D, Alicat Scientific, Inc., USA) was employed. A high-efficiency particulate absorbing (HEPA) filter in conjunction with a water bubbler was used to prevent particles' elutriation into the atmosphere.

The solenoid was installed under the column, as shown in Fig. 1. It was composed of an iron core with an inner diameter of 50 mm, a thickness of 5 mm, and 3000 wires of copper with a diameter of 0.35 mm wrapping around the iron core. The inlet voltage of the solenoid and the strength of the magnetic field were controlled using an electric valve (ToYo MST-1kVA). In this study, a 220 V, 50 Hz urban voltage was used as the variac input, and a voltage of 0 to 220 V with the same frequency was used as the solenoid input.
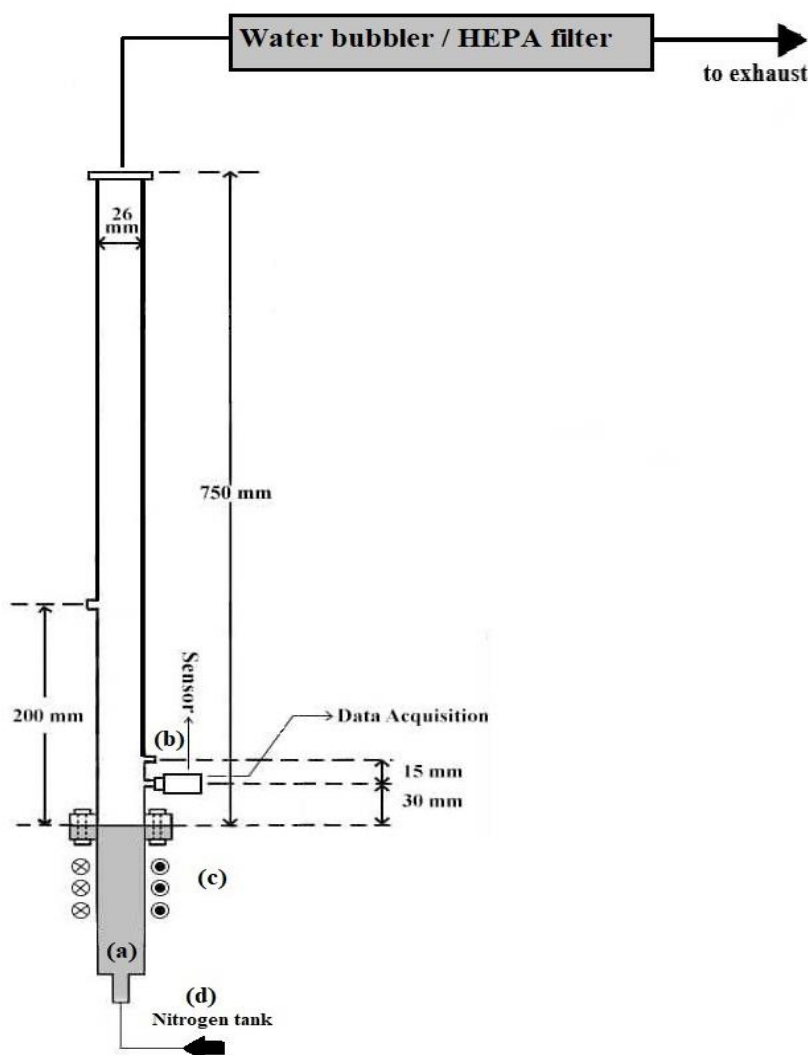

Fig.1. Schematic of the experimental set-up (a) wind box (b) sampling ports (c) solenoid (d) mass flow controller and nitrogen supply tank

Titanium oxide nanopowder in the anatase phase was used as the principal powder with a mean diameter of 21 nm and a bulk density of 420 kg/m^3 (provided by Nanostructured & Amorphous Materials). In addition, ferromagnetic iron (III) oxide nanoparticles were employed as the magnetic agents with a size distribution of 20-30 nm and a bulk density of 840 kg/m^3 (provided by US-nano). To break the initial agglomerates formed during filling and transferring powder, a certain procedure was followed before each test. The powder was first sieved through a screen with a pore size of 275 µm. Thereafter, a high gas flow was injected

into the bed to break the agglomerates and prevent clogging. The bed pressure fluctuations were measured using a piezoresistive pressure sensor (model 7261, Kistler© Co., Switzerland). The response time of the sensor was less than 1 ms with an accuracy of 0.5% of the full scale. There are detailed descriptions of the experiments and equipment in a previous study [19].

Data Analysis

Wavelet transform was first proposed to cover the drawbacks of fast Fourier transform analysis. Wavelet transform decomposes a time series into a group of functions, $\psi_{jk}(t)$, that comes from N adjusting mother wavelet function $\psi(t)$, using two parameters according to the following equation:

$$\psi_{jk}(t) = \frac{1}{\sqrt{|j|}} \sum_{i=1}^{N} \psi \left(\frac{t-k}{j} \right) \tag{1}$$

Here, j and k are the parameters related to scale and translation of the function $\psi(t)$, respectively. These parameters are applied to localize the frequency and time domain of the function, respectively. Multi-resolution theory suggests that a specific signal can be decomposed at the j level into two groups of orthogonal sub-signals, approximation (A_j) and details (D_j). These sub-signals represent the main signal at different scales and resolutions. Therefore, their combination reconstructs the primary signal:

$$P'(i) \approx A_j(i) + \sum_{j=1}^{J} D_j(i) \tag{2}$$

The energy of the main signal, the detail, and the approximate sub-signals can be calculated, respectively, from:

$$E = \sum_{i=1}^{N} |P(i)|^2 = \sum_{i=1}^{N} |A_j(i)|^2 + \sum_{i=1}^{N} |D_j(i)|^2 \tag{3}$$

$$E_j^D = \sum_{i=1}^{N} |D_j(i)|^2, \tag{4}$$

$$E_j^A = \sum_{i=1}^{N} |A_j(i)|^2, j = 1,2,3,\dots,J. \tag{5}$$

A crucial step in obtaining good accuracy with wavelet analysis is to choose the proper mother wavelet [20]. In this work, the Daubechies mother wavelet was used. To determine the proper order of the Daubechies function, reconstruction errors were calculated for 12 different orders of Daubechies, and the second-order function, which had the minimum reconstruction error, was chosen for further analysis. The reconstruction error is the difference between the original time series and the reconstructed one from the decomposed sub-signals. The proper level of decomposition was determined by calculating the amount of information that remained in the decomposed detail sub-signals. For this purpose, normalized Shannon entropy was used for obtaining the level of decomposition [21]. The level with the minimum Shannon entropy was chosen as the proper level of decomposition. In this study, the proper level of decomposition was determined to be 8.

Results and Discussion

The decomposed sub-signals obtained from wavelet transform were analyzed using the method proposed by Tahmasebpour et al. [22] for identifying the hydrodynamic structure in the bed. Large-scale phenomena (bubbles) in the bed behave in a more deterministic behavior and are considered macrostructure. These structures are represented by A(8), D(8), D(7), and D(6) sub-signals. The microstructure consists of the noises of measurement systems in the fluidization of nanoparticles. These small-scale phenomena exhibit a more stochastic behavior in the bed and are represented by D(1) and D(2) sub-signals. Meso structures are agglomerates in the bed. Due to the movement of the agglomerates and their size distribution, these structures have a higher frequency compared to macrostructures, but lower than microstructures in the PSD analysis of pressure fluctuations. Therefore, mesostructures include the sub-signals represented by D(3), D(4), and D(5) sub-signals. As the microstructures provide no valuable information about the hydrodynamics of the nanoparticle fluidized beds, they were merged with mesostructures in the present study and are considered finer structures. The frequency range of the hydrodynamic structures in the bed is reported in Table 1.

Table 1. The frequency range of the hydrodynamic range

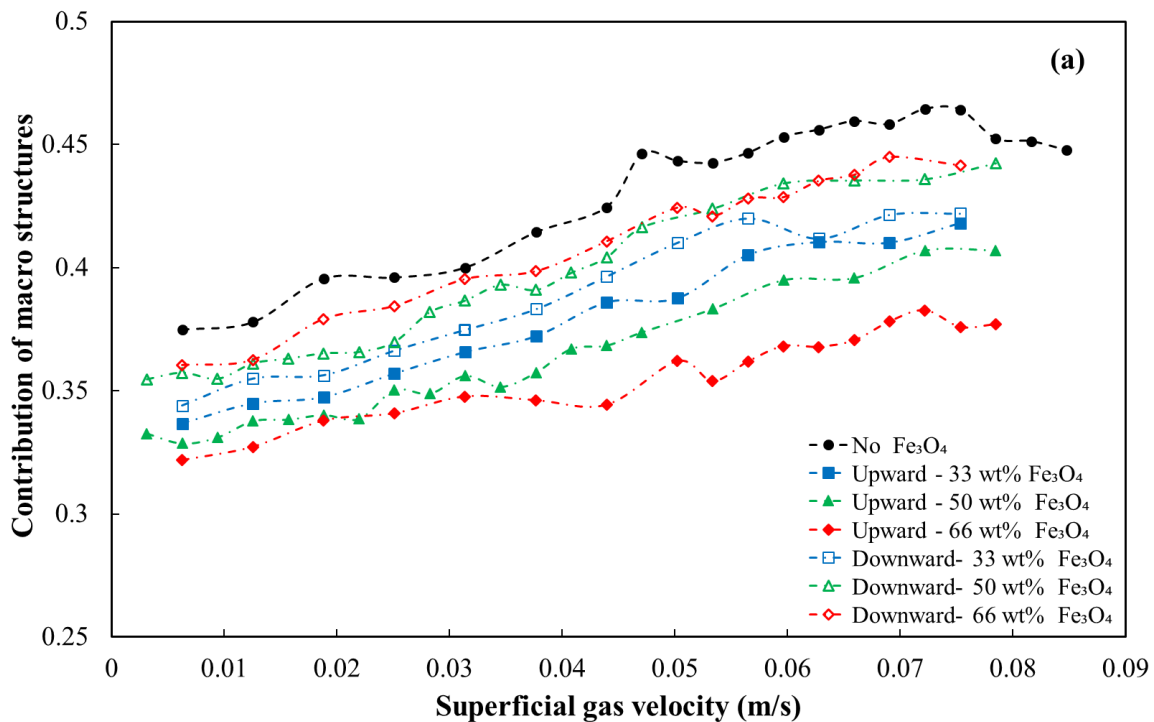| Finer structures	Macrostructure
12.5 - 200 Hz	0 - 12.5 Hz

Fig. 2 shows the energy of hydrodynamic structures for different directions of the magnetic field at 400 Gauss and various superficial gas velocities. The energy contribution of each structure is determined as the ratio of the total energy of the constitutive sub-signals to the total energy of the primary signal ($\sum_j E_j^D /E$). As can be seen in this figure, with increasing the gas velocity the energy contribution of micro and mesostructures decreases, and the contribution of macrostructure increases in the bed. With increasing the gas velocity, more bubbles are formed in the bed and, as a result, the energy contribution of the macrostructure increases, as can be seen in Fig. 2a. As the contribution of the large-scale phenomena (bubbles) increases, the contribution of finer structures (particle and agglomerates interactions) decreases. This means that at high gas velocities, the hydrodynamics is affected more by the bubbles than the smaller phenomena.

It can be seen in Fig. 2a at the field strength of 400 Gauss, that the contribution of macro structures decreases by applying the magnetic field (mainly due to the effect of vibration, then the magnetic force), which indicates a decrease in the bubble size. This figure also shows that the direction of the magnetic field has a minor effect on the energy of macrostructures. But in general, the upward produces smaller bubbles compared with the downward field by increasing the mobility and interaction between agglomerates. An increase in the mass fraction of the magnetic particles enhances the effect of the magnetic field. For the upward/downward direction of the field, higher mass fractions of Fe_3O_4 nanoparticles form smaller/larger bubbles in the bed. Smaller bubbles are formed in the bed with smaller agglomerates which is the case for the upward direction of the magnetic field.

Fig. 2b shows that the energy contribution of mesostructures is higher when the magnetic field is applied, indicating that there is a higher number of agglomerates in the bed compared to when the magnetic field is off. The energy contribution of mesostructures is higher for the upward field direction since agglomerates are smaller in the presence of upward fields when compared with the downward. Increasing the mass fraction of the ferromagnetic nanoparticles enhances the effect of the magnetic field on fluidization. There is no meaningful difference between the contributions of microstructures in different fluidization conditions, as shown in Fig. 2c. The micro-scale part of the signal in the fluidization of nanoparticles presents the measurement noises. Interactions between particles for nanopowders are very weak and have a negligible effect on the hydrodynamics compared to agglomerates and bubbles. In other

words, the effect of the movement of individual particles cannot be detected. As a result, as can be concluded from the trends in Fig. 2c, the energy contribution of microstructure presents no valuable information about the hydrodynamics of fluidization.

Fig. 3 shows the energy contribution of the hydrodynamic structures at 582 Gauss magnetic field strength at various superficial gas velocities. As can be seen in this figure, the energy contribution of macro/mesostructures decreases/increases upward direction the macro and the with increasing the superficial gas velocity, which indicates the formation of more bubbles in the bed. Fig. 3a shows that, compared to no magnetic field, the energy of macro structures increases/decreases for a downward/upward magnetic field by increasing the fraction of magnetic particles (i.e., increasing the magnetic force exerted on the bed materials). Unlike Fig. 2 (lower field strength of 400 Gauss), at this field strength (582 Gauss), the magnetic force is larger than the vibration, and its direction has a meaningful effect on the hydrodynamics. Higher/lower energy of macrostructures in Fig. 3a than in the absence of magnetic force indicates the existence of larger/smaller bubbles when a strong downward/upward magnetic field is applied to the bed. The corresponding trend can be seen in Fig. 3b about mesostructures in which lower/higher energy of these structures (compared to no magnetic force case) suggest lower/higher mobility of agglomerates (larger/smaller agglomerates) in the presence of downward/upward magnetic field and increasing the fraction of magnetic nanoparticles in the bed enhances this effect.
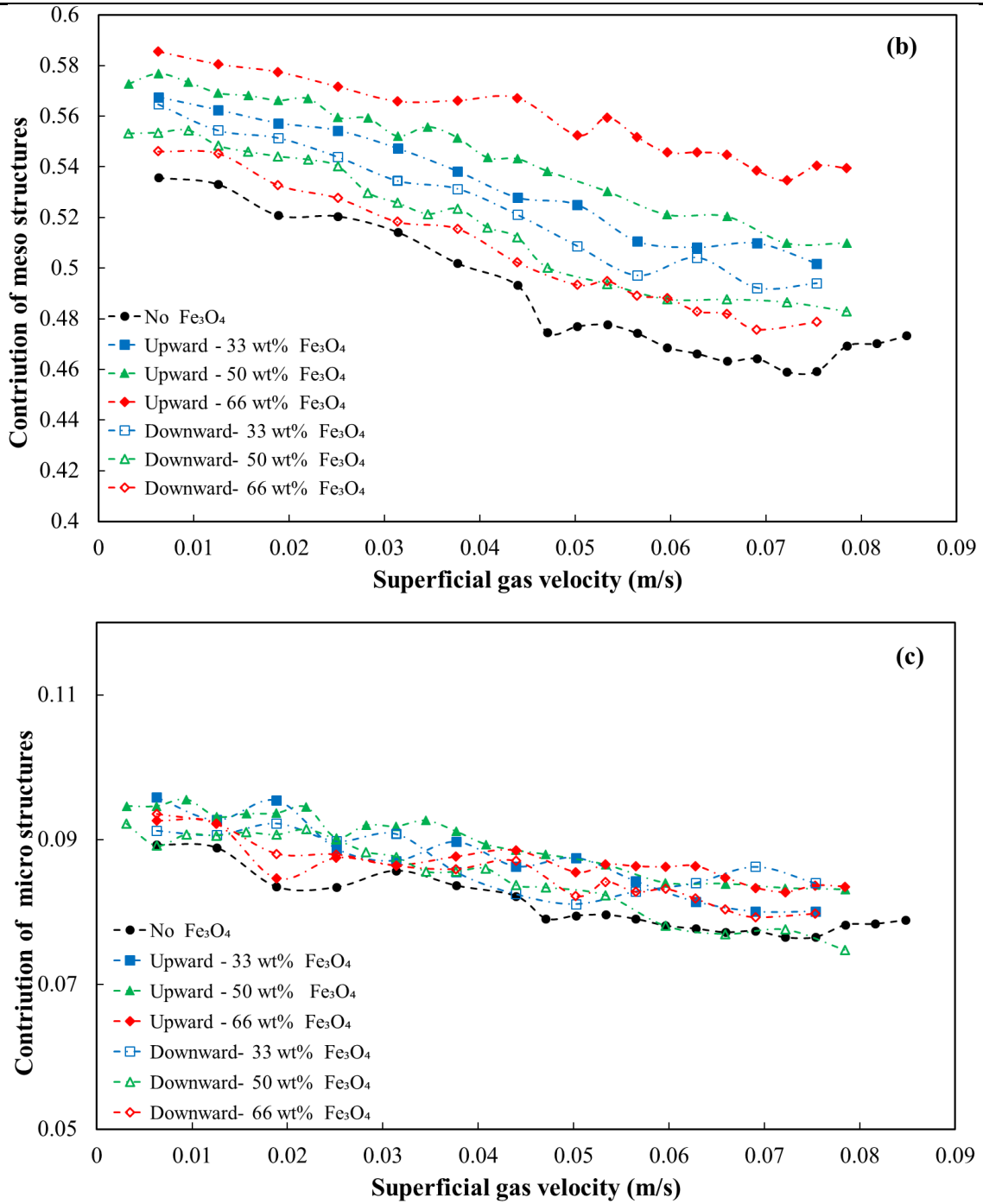

(a)

Legend:
- No Fe_3O_4
- Upward - 33 wt% Fe_3O_4
- Upward - 50 wt% Fe_3O_4
- Upward - 66 wt% Fe_3O_4
- Downward- 33 wt% Fe_3O_4
- Downward- 50 wt% Fe_3O_4
- Downward- 66 wt% Fe_3O_4

Y-axis: Contribution of macro structures
X-axis: Superficial gas velocity (m/s)

Fig. 2. Contribution of each hydrodynamic structure against gas superficial velocity at 400 Gauss magnetic field strength (a) macro structures (b) mesostructures (c) microstructures
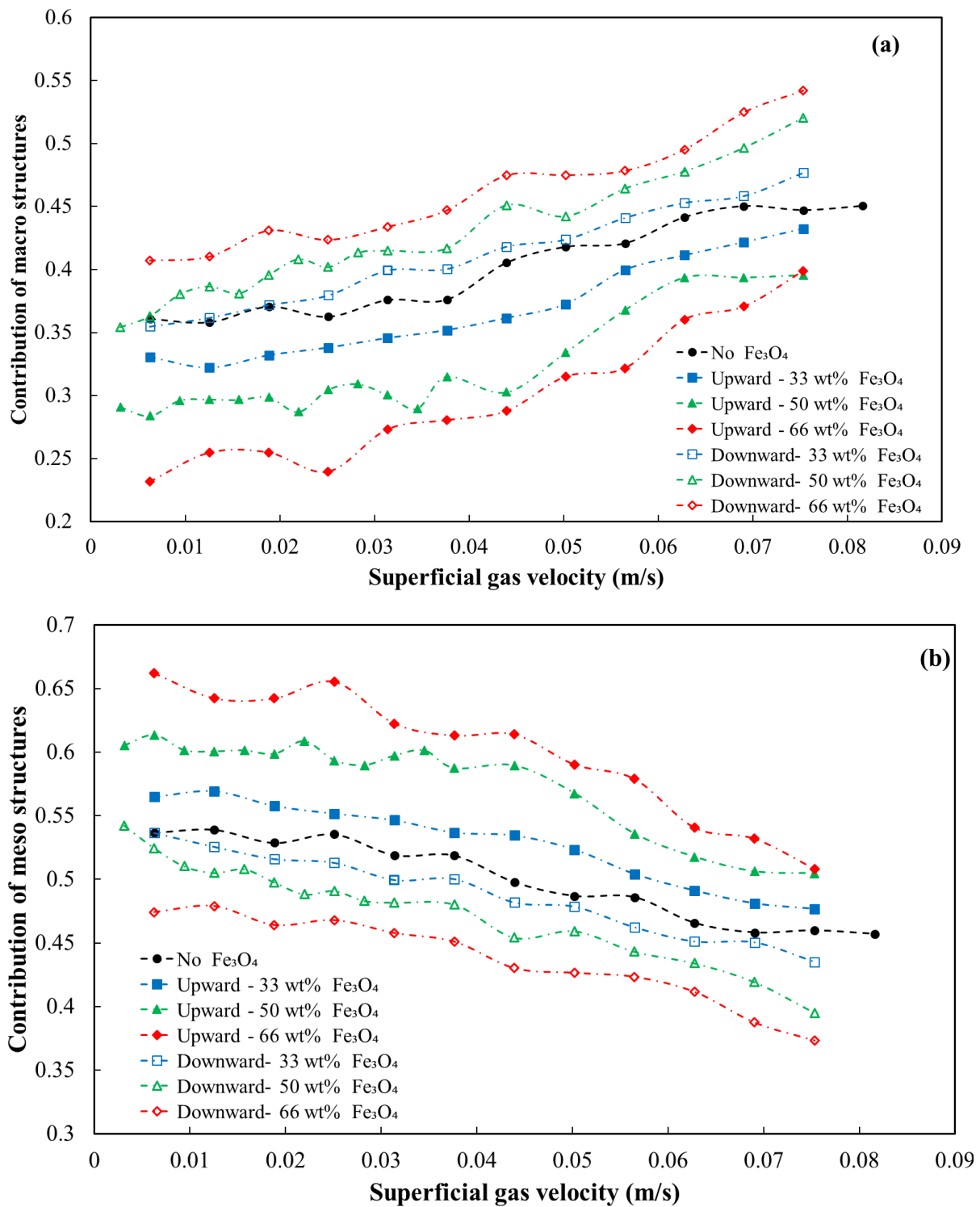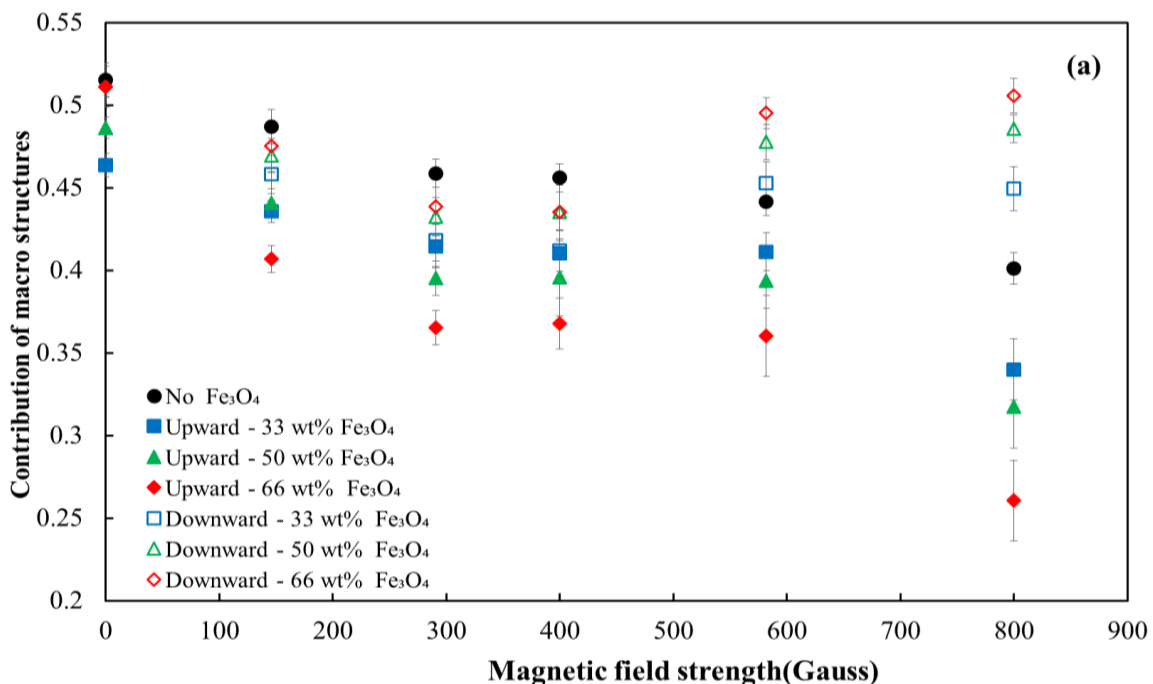
Fig. 3. Contribution of energy of hydrodynamic structures against superficial gas velocity at 582 Gauss magnetic field strength (a) macro structures (b) mesostructures

Due to the increased effect of the magnetic force on fluidization, the trend is different for upward and downward fields. At low magnetic field strengths, the vibration of the solenoid has a major effect, and combined with the magnetic force, they improve the quality of fluidization (Fig. 2). At higher magnetic field strengths (Fig. 3), the magnetic force applied to the bed grows larger than the vibration and results in the movement and interaction of the ferromagnetic

particles in the upward/downward direction to increase/decrease. This phenomenon can be seen by the change in the energy contribution of these cases that causes the difference in trends observed in Figs. 2 and 3, such that the data point for "No Fe_2O_3 particles" in Fig 3 lies between upward and downward cases while in Fig. 2 they are at the top.

Fig. 4 shows the variation of the energy of hydrodynamic structures against the magnetic field strength at the superficial gas velocity of 6.27 cm/s. It is shown in Fig. 4a that the energy contribution of macro structures in the case of the upward direction of the magnetic field decreases with increasing the field strength and is always higher than no magnetic force acting on the bed materials. This trend suggests that smaller bubbles are formed as the strength of the upward magnetic field strength is increased. In the case of a downward field, the same trend exists for field strength less than 400 Gauss, while the energy contribution of macro structures becomes increasing and higher than no magnetic force at fields greater than 400 Gauss. In this case, at field strengths of 400 Gauss or less, the effect of vibration on the hydrodynamics is stronger than the magnetic force. At higher downward magnetic field strengths, however, the magnetic force acting on the bed materials becomes greater than that from the vibration and larger agglomerates are formed in the bed due to reduced mobility and movement of the particles. Consequently, larger bubbles are formed in this situation which increases the energy of macrostructures. A reverse trend can be observed in Fig. 4b since an increase in the fractional energy of macro structures results in a decrease in the fractional energy of finer structures and vice versa.
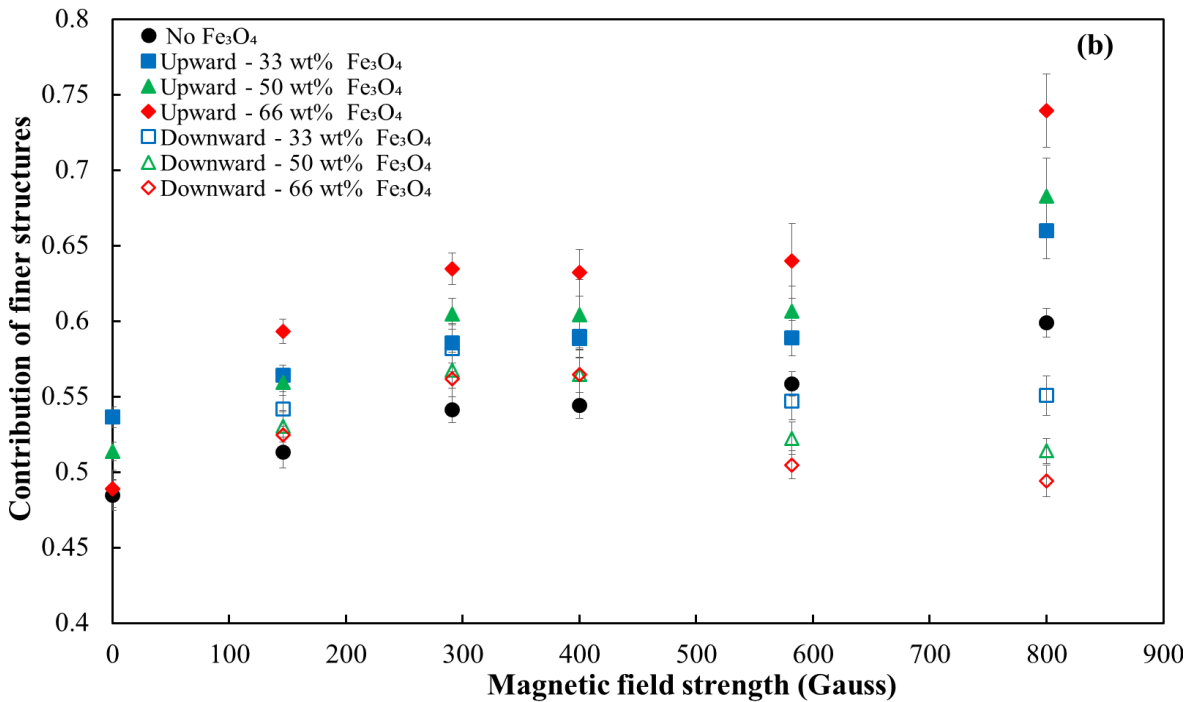
Fig. 4. The energy contribution of hydrodynamic structures against magnetic field strength at the superficial gas velocity of 6.27 cm/s (a) Macro structures (b) Finer structures (meso + micro)

Conclusion

The effect of magnetic field strength and direction on the fluidization of titanium oxide nanoparticles was studied in this study. Pressure fluctuations of the bed were decomposed to a set of sub-signals through the wavelet transform. The main hydrodynamic structures were identified through the evaluation of determinism of the sub-signals. Energy analysis of the sub-signals suggested that the magnetic field affects the mesostructure (agglomerates) the most. An increase in the energy contribution of finer structures (meso and micro) indicated the increase in the mobility of the agglomerates (interaction and formation) in the bed.

Results showed that at low field strengths less than 400 Gauss, the vibration of the solenoid improved the fluidization quality, regardless of the field direction, by increasing the energy contribution of finer structures. An increase in the energy contribution of finer structures for field strength less than 400 Gauss is due to the vibration effect of the solenoid that increases the interaction between agglomerates in the bed. At field strengths greater than 400 Gauss, as the magnetic force grows stronger, the magnetic field affects the movement of ferromagnetic particles in the bed as well as their interactions with each other and with other particles in the bed. At high magnetic field strengths, the field-effect associated with the vibration effect further improves the fluidization quality for upward direction by increasing the interactions in the bed and decreasing the size of agglomerates. This effect can be seen by the increase in the contribution of finer structures and the decrease in the contribution of the energy of macro structures indicates the formation of smaller bubbles size for the upward direction of the field.

Applying the downward field improves the fluidizing quality at strengths less than 400 Gauss, and decreases deteriorates the quality at higher strengths. At higher field strengths, the magnetic force is imposed on the bed in the reverse direction of the gas flow and causes resistance against fluidization. This effect can be seen by the decrease of the energy contribution of the finer structures in this situation. Also, an increase in the energy of macro

structures was observed at high field strength for the downward direction, which indicates the formation of larger bubbles in the bed for such fluidization mode.

Increasing the mass fraction of Fe_3O_4 particles in the bed improves the quality of fluidization for the upward field by increasing the number of particles that receive the magnetic force that increases the interaction in the bed. For the downward field case, as more particles receive the magnetic force at high field strength, the downward force affects the fluidization toward preserving the packed bed of particles.

Nomenclature

$A_j(i)$	Approximate Sub-Signal
$D_j(i)$	Detail Sub-Signal
E	Energy of the Signal (Pa^2/Hz)
E_j^A	The energy of Approximation Coefficient (Pa^2/Hz)
E_j^D	The energy of Detail Coefficient (Pa^2/Hz)
j	Index for Rescale in Wavelet Transform
K	Index for Shift in Wavelet Transform
$P(i)$	Measured Pressure Signal
N	Number of Data Points
$P'(i)$	Reconstructed Signal
U	Superficial Gas Velocity (m/s)
$\psi(t)$	Mother Wavelet Function

References

[1] Van Ommen JR, Valverde JM, Pfeffer R. Fluidization of nanopowders: a review. Journal of nanoparticle research. 2012;14(3):1-29.

[2] Zhao Z, Liu D, Ma J, Chen X. Fluidization of nanoparticle agglomerates assisted by combining vibration and stirring methods. Chemical Engineering Journal. 2020;388:124213.

[3] Mostoufi N. Revisiting classification of powders based on interparticle forces. Chemical Engineering Science. 2021;229:116029.

[4] Geldart D. Types of gas fluidization. Powder technology. 1973;7(5):285-92.

[5] Esmailpour AA, Mostoufi N, Zarghami R. Effect of temperature on fluidization of hydrophilic and hydrophobic nanoparticle agglomerates. Experimental Thermal and Fluid Science. 2018;96:63-74.

[6] Seville J, Willett C, Knight P. Interparticle forces in fluidisation: a review. Powder Technology. 2000;113(3):261-8.

[7] Shabanian J, Jafari R, Chaouki J. Fluidization of ultrafine powders. International review of chemical engineering. 2012;4(1):16-50.

[8] Yao W, Guangsheng G, Fei W, Jun W. Fluidization and agglomerate structure of SiO2 nanoparticles. Powder Technology. 2002;124(1-2):152-9.

[9] Liu Y, Ohara H, Tsutsumi A. Pulsation-assisted fluidized bed for the fluidization of easily agglomerated particles with wide size distributions. Powder Technology. 2017;316:388-99.

[10] An K, Andino JM. Enhanced fluidization of nanosized TiO2 by a microjet and vibration assisted (MVA) method. Powder Technology. 2019;356:200-7.

[11] Hoorijani H, Zarghami R, Nosrati K, Mostoufi N. Investigating the hydrodynamics of vibro-fluidized bed of hydrophilic titanium nanoparticles. Chemical Engineering Research and Design. 2021;174:486-97.

[12] Vahdat MT, Zarghami R, Mostoufi N. Fluidization characterization of nano-powders in the presence of electrical field. The Canadian Journal of Chemical Engineering. 2018;96(5):1109-15.

[13] Karimi F, Haghshenasfard M, Sotudeh-Gharebagh R, Zarghami R, Mostoufi N. Enhancing the fluidization quality of nanoparticles using external fields. Advanced Powder Technology. 2018;29(12):3145-54.

[14]   van Ommen JR, Sasic S, van der Schaaf J, Gheorghiu S, Johnsson F, Coppens M-O. Time-series analysis of pressure fluctuations in gas–solid fluidized beds – A review. International Journal of Multiphase Flow. 2011;37(5):403-28.

[15]   Zarghami R, Mostoufi N, Sotudeh-Gharebagh R. Nonlinear characterization of pressure fluctuations in fluidized beds. Industrial & engineering chemistry research. 2008;47(23):9497-507.

[16]   Tamadondar MR, Zarghami R, Tahmasebpoor M, Mostoufi N. Characterization of the bubbling fluidization of nanoparticles. Particuology. 2014;16:75-83.

[17]   Farahani AA, Norouzi HR, Zarghami R. Mixing of nanoparticle agglomerates in fluidization using CFD-DEM at ABF and APF regimes. Chemical Engineering Research and Design. 2021;169:165-75.

[18]   Liu H, Wang S. Fluidization behaviors of nanoparticle agglomerates with high initial bed heights. Powder Technology. 2021;388:122-8.

[19]   Hoorijani H, Zarghami R, Mostoufi N. Studying the effect of direction and strength of magnetic field on fluidization of nanoparticles by recurrence analysis. Advanced Powder Technology. 2022.

[20]   Rodrigues A, Dmello G, Pai P. Selection of Mother Wavelet for Wavelet Analysis of Vibration Signals in Machining. Journal of Mechanical Engineering and Automation 2016, 6(5A): 81-85.

[21]   Rioul O, Vetterli M. Wavelets and signal processing. IEEE signal processing magazine. 1991;8(4):14-38.

[22]   Tahmasebpoor M, Zarghami R, Sotudeh-Gharebagh R, Mostoufi N. Characterization of fluidized beds hydrodynamics by recurrence quantification analysis and wavelet transform. International journal of multiphase flow. 2015;69:31-41.